Click Here for Full Article

Climatology and summer energy and water balance of polygonal tundra in the Lena River Delta, Siberia

Julia Boike,[1] Christian Wille,[1,3] and Anna Abnizova[2]

[1] Meteorological and soil temperature and moisture data for the period 1998–2005 are presented from a long term monitoring station in the central Lena River Delta at 72°N, 126°E. The investigation site, Samoylov Island, is situated in the zone of continuous permafrost and is characterized by wet polygonal tundra. The summer energy and water balance of the tundra was analyzed for the dry year 1999 and the wet year 2003. The summer water balance of the tundra was found to be mainly controlled by precipitation. The partitioning of the available energy was controlled by precipitation via the soil moisture regime, and by the synoptic weather conditions via radiation and the advection of maritime cold or continental warm air masses. In 2003, regular high precipitation resulted in a constant recharge of polygonal ponds. Of the available energy, 61% were partitioned into latent heat flux and 17% into ground heat flux; hence, the tundra behaved like a typical wetland. In 1999, low precipitation resulted in a loss of polygonal pond waters and a drying of upper soil layers. This led to lower latent heat flux (31% of available energy), higher ground heat flux (29%), and a considerably higher soil thaw depth compared to 2003. Surface and subsurface water flow had a significant influence on the tundra water balance. In 2003, the formation of new surface flow channels through thermo-erosion was observed, which is expected to have a strong and lasting influence on the hydrologic system of the tundra.

Citation: Boike, J., C. Wille, and A. Abnizova (2008), Climatology and summer energy and water balance of polygonal tundra in the Lena River Delta, Siberia, *J. Geophys. Res.*, *113*, G03025, doi:10.1029/2007JG000540.

1. Introduction

[2] The prediction of the response of land surface water and energy fluxes to environmental change is a major challenge for experimentalists and climate modelers alike. Several studies documented potential changes in the Arctic hydrologic system. These include lake drainage through thawing permafrost [*Smith et al.*, 2005; *Yoshikawa and Hinzman*, 2003] and changes in Siberian river runoff [*Yang et al.*, 2002; *Berezovskaya et al.*, 2004, 2005]. Quantifying the coupled surface energy and water balance is a prerequisite to understand the causes of changes in these systems. Measurements of the fluxes between the terrestrial and atmospheric systems are difficult to obtain. *Eugster et al.* [2000] state that one of the most important uncertainties for assessment of susceptibility and vulnerability of the boreal and Arctic are the difficulties in measuring surface fluxes. Some of the experimental problems include the remoteness of Arctic sites and extreme weather conditions which can prohibit the use of precise flux measurements techniques

such as the eddy covariance technique, and the great variety of measurement and analysis techniques used by different studies [e.g., *Eugster et al.*, 2000; *Lynch et al.*, 1999].

[3] According to *Vörösmarty et al.* [2001], the understanding of the seasonal and spatial variability of the pan Arctic water balance is one major open question. However, it is recognized that wet tundra environments represent a major contribution to land-atmosphere exchanges of water, energy, carbon and greenhouse gases [*Chapin et al.*, 2000]. The tundra environments are underlain by continuous permafrost which creates an impermeable layer and, together with low topographic gradients, results in numerous ponds and lakes (wetland). The drainage network is restricted downward by frozen ground, and evapotranspiration is a major mechanism of water loss. Several studies have been carried out recently to characterize the morphology and understand the developmental factors of small, patchy wetlands in the Canadian High Arctic [e.g., *Woo and Young*, 2003; *Young and Woo*, 2000]. The existence of wetlands requires a positive water balance associated with precipitation and evapotranspiration regimes and interactions between surface and groundwater flows [*Woo and Young*, 2006]. In the Alaskan Arctic close to Prudhoe Bay, evapotranspiration exceeds precipitation during the thaw period, leading to a general drying of the watershed [*Mendez et al.*, 1998]. In the study of extensive wetland in a low gradient Putuligayuk River watershed in northern Alaska, *Bowling et al.* [2003] identified meltwater as the primary source of the

---

[1]Periglacial Section, Alfred Wegener Institute for Polar and Marine Research, Potsdam, Germany.
[2]Department of Geography, York University, Toronto, Ontario, Canada.
[3]Now at Institute of Botany and Landscape Ecology, University of Greifswald, Greifswald, Germany.
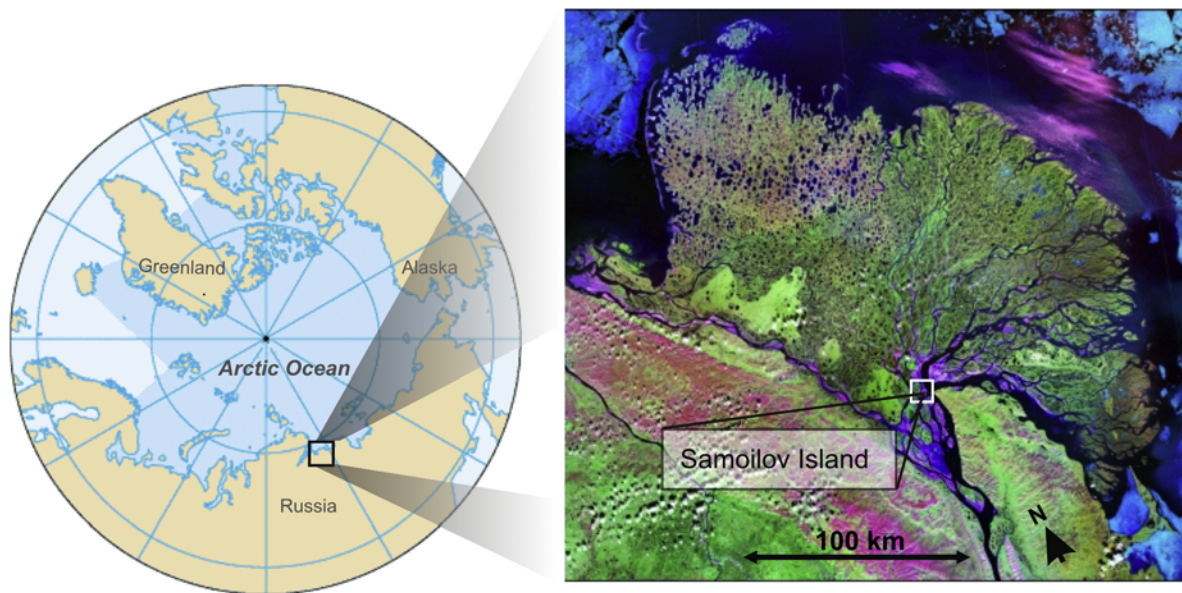
Figure 1. Circumpolar map showing the Lena River Delta in Siberia. The location of the investigation area within the delta is marked by a white square. The closest settlement is Tiksi, about 110 km southeast of the site. Satellite image provided by Statens Kartverk, UNEP/GRID-Arendal and Landsat, 2000.

wetland's water budget. In contrast to these well researched sites in the North American Arctic, there is a complete lack of long-term energy balance data from Siberia and a poor representation in the rest of the circumpolar boreal and Arctic zones [*Eugster et al.*, 2000].

[4] This paper's research site is located in the Lena River Delta, which is the largest river delta in northern Asia and one of the richest areas in the Arctic for both species diversity and breeding densities of migratory birds [*Gilg et al.*, 2000]. The delta channels one of the largest fluvial contributions of water to the Laptev Sea [*Yang et al.*, 2002; *Spielhagen et al.*, 2005]. The goals of this paper are to (1) characterize the site's climatology for the years 1998–2005, and (2) quantify and discuss the coupled energy and water balance for a dry (1999) and a wet summer (2003) at a polygonal tundra site. Thus the study aims to display differences and similarities in the response of the energy and water balance to climate variability.

2. Study Site

2.1. Geography

[5] The investigation site is located on Samoylov Island (72°22′N, 126°30′E, Figure 1), one of the 1500 islands within the Lena River Delta, in one of the main river channels approximately 120 km south of the Arctic Ocean. The Lena Delta is located in the zone of continuous permafrost with permafrost depths ranging from 500–600 m [*Zhang et al.*, 1999; *National Snow and Ice Data Center* (*NSIDC*), 2003]. The western part of the island (3.4 km^2) represents a modern floodplain with an elevation of 1 to 5 m a.s.l., which is flooded annually in spring. The eastern part of the island (4.1 km^2), where instruments were set up, is composed of sediments of the Late-Holocene river terrace [*Schwamborn et al.*, 2002] and is characterized by wet polygonal tundra. Its elevation ranges from 10 to 16 m

a.s.l., and only small parts of it are flooded during the annual spring flood. The macrorelief of the eastern part of Samoylov Island is level with slope gradients <0.2%. The only abrupt changes in elevation, of up to 2.5 m, are associated with the shorelines of the larger lakes.

[6] The surface of the terrace is structured by a microrelief with elevation differences of up to 0.5 m over a few meters distance, which is caused by the genesis of low-centered ice wedge polygons (Figure 2). In the depressed polygon centers, drainage is strongly impeded due to the underlying permafrost, and water-saturated soils or small ponds occur. In contrast, the elevated polygon rims are characterized by a moderately moist water regime. The typical soil types are *Typic Historthels* in the polygon centers and *Glacic* or *Typic Aquiturbels* at the polygon rims, respectively [*United State Department of Agriculture* (*USDA*), 1998]. The polygon centers have a water level near the soil surface and a silty sand soil texture with anaerobic accumulation of organic matter. The soils of polygon rims are characterized by a silty and loamy sand texture with low organic matter content due to oxic conditions and low water levels [*Wagner et al.*, 2005]. Measured laboratory soil porosities range between 0.52 and 0.68 [*Kutzbach*, 2006]. The vegetation in the polygon centers and rims is composed of a moss and lichen strata of about 5 cm thickness and a vascular plants strata of 20–30 cm height [*Kutzbach et al.*, 2004]. The prevailing vascular plant is the hydrophilic sedge *Carex aquatilis*, which is generally dominant in the polygon centers (25%) and found to a lesser extent on polygon rims (8%). Apart from *C. aquatilis*, the vegetation of polygonal centers includes the mosses *Limprichtia revolvens* and *Meesia longeseta*. The polygon rims are dominated by mesophytic dwarf shrubs *Dryas octopetala* and the mosses *Hylocomnium splendens* and *Timmia austriaca* [*Kutzbach et al.*, 2004]. More detailed information on soil types and vegetation of the polygonal tundra
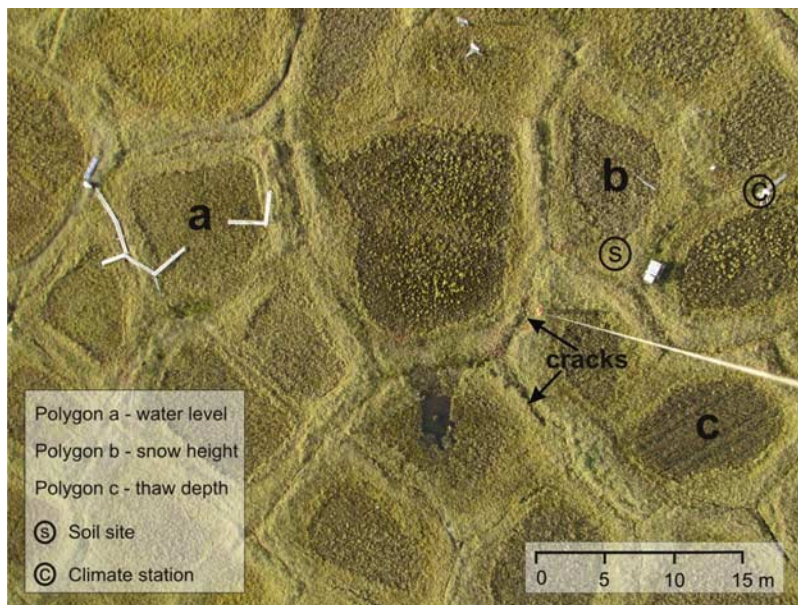
Figure 2. Aerial picture of experimental sites on the polygonal tundra on Samoylov, taken in August 2006. The ice wedge polygonal network is clearly visible. The low center polygons are usually water filled, while the surrounding elevated rims appear drier. Note that the rims above the ice wedges are divided by surficial cracks.

on Samoylov Island is given by *Pfeiffer et al.* [2002], *Fiedler et al.* [2004], and *Kutzbach et al.* [2004].

2.2. Climate Characteristics

[7] The Lena Delta region has a dry continental Arctic climate, characterized by very low temperatures and low precipitation. The mean annual air temperatures and total rainfall for the years 1961–1999 measured by the meteorological station Tiksi, 110 km south-east of Samoylov, are −13.6°C and 319 mm, respectively [*ROSHYDROMET*, 2006]. Polar day lasts from 7 May to 7 August and polar night from 15 November to 28 January. The snowmelt typically starts at around the beginning of June and the growing season lasts from the middle of June to the middle of September. About 45% of the precipitation falls as rain during the growing season. During spring, summer and autumn, the weather at Samoylov Island is characterized by the rapid change between the advection of arctic cold and moist air masses from the north and continental warm and dry air masses from the south. The mean annual temperature at the top of the permafrost is −10.1°C, which is extremely cold compared to other Arctic sites. Colder permafrost is only encountered on the Taymyr Peninsula to the North-West of the Lena River Delta and on the Canadian Arctic Archipelago [*Natural Resources Canada*, 1995; *Kotlyakov and Khromova*, 2002]. In comparison, the top of permafrost temperature on Svalbard is much higher, about −3°C [*Boike et al.*, 2003b].

3. Methods

3.1. Experimental Setup

[8] A soil profile located at a polygonal rim site was instrumented in August 1998 for the monitoring of soil temperature and soil water content. Soil temperatures were recorded using thermistors (107, Campbell Scientific Ltd., UK). The thermistors were calibrated at 0°C so that the absolute error was less than 0.02 K over the temperature range ±30°C. Liquid water content was calculated from time domain reflectometry measurements (Tektronix 1502, TDR100, CR10X, Campbell Scientific Ltd., UK) using the semiempirical mixing model of *Roth et al.* [1990]. The accuracy of the measurement of volumetric water content by TDR is estimated to be between 2 to 5% volumetric water content (VWC), while the precision is better than 0.5% VWC [*Boike and Roth*, 1997].

[9] A meteorological station was set up within 10 m of the instrumented soil site. The variables measured were air temperature and relative humidity at heights of 0.5 and 2.0 m above the ground (MP103A, Rotronic AG, Switzerland), wind speed and direction (05103, R.M. Young Company, USA), snow depth (SR50, Campbell Scientific Inc., USA), and rainfall (52203, R.M. Young Company, USA). Net radiation was measured initially using a Q7 net radiometer (REBS, USA), which was replaced by an NR-Lite net radiometer (Kipp & Zonen B.V., Netherlands) in August 2000. Both sensors were installed during the period August 2001 to August 2002 for comparison. A linear fit of net radiation readings showed that, compared to the NR-Lite sensor, the Q7 overestimated negative net radiation and underestimated positive net radiation by typically 7% and 8%, respectively. Hourly data collection of soil and climate data began in August 1998. Because of technical problems, several gaps in the data exist, most notably during May 2000 to March 2001, and January to July 2003. The soil instruments were replaced by new sensors during the summer of 2002. During this process, soil and climate stations were moved to a new neighboring site, approximately 30 m northeast from the first site (site s, Figure 2).

[10] Water level was measured in 5 wells reinforced by perforated PVC pipes which were located in a polygon near

the climate station (polygon a, Figure 2, *Wagner et al.* [2003]). The change of (surface and subsurface) water storage ΔS_{meas} was calculated as the relative change of water level in mm. The depth of the thawed active layer was determined from soil temperature profile measurements.

3.2. Energy Balance Calculation

[11] A simple volume energy balance of the seasonally thawing and freezing soil may be formulated as (adapted from *Boike et al.*, 2003a):

$$Q_n + Q_h + Q_e + Q_r = Q_g \qquad (1)$$

where Q_n is the net radiation, Q_h and Q_e are turbulent fluxes of sensible and latent heat, Q_r is the heat flux supplied by rain, and Q_g is the ground heat flux. The atmospheric fluxes on the left side of the equation are defined as positive when they are directed toward the soil surface (energy gain). The net radiation Q_n is measured by a net radiometer, Q_r is calculated using rainfall rate and the difference between air and soil temperature at 6 cm depth, and Q_e, and Q_g are estimated as described below. The turbulent sensible heat flux Q_h is calculated as the remainder in the balance. Assuming an error of Q_g and Q_n of $\pm15\%$, the error of Q_e and Q_h by error propagation was estimated to be about $\pm21\%$.

[12] The latent heat flux Q_e was calculated using the model developed by *Priestley and Taylor* [1972], which has been successfully applied in various settings in the Arctic [*Mendez et al.*, 1998; *Rouse*, 1990; *Marsh et al.*, 1981; *Woo and Marsh*, 1990]:

$$Q_e = \frac{\alpha_{PT}\Delta VP(T)(Q_n - Q_g)}{\Delta VP(T) + \gamma} \qquad (2)$$

[13] Here $\Delta VP(T)$ is the slope of the saturation vapor pressure-temperature curve, γ is psychrometric constant, and α_{PT} is a parameter expressing the ratio of actual to equilibrium evapotranspiration. The value of α_{PT} for our study site was derived empirically by application of the Bowen Ratio - energy balance method (BREB) to 1999 and 2003 data sets to approximate the ratio of actual to equilibrium evapotranspiration [*Eichinger et al.*, 1996]. To estimate the relative humidity at the soil surface the relation between water potential and relative humidity was used [*Campbell*, 1985; *Stewart and Broadbridge*, 1999]. Estimation of water potential using volumetric soil moisture relationship was performed following *Hinzman et al.* [1998]. The average estimated value of α_{PT} in 2003 was 1.26, which is a value generally accepted for saturated surfaces [e.g., *Rouse et al.*, 1977; *Stewart and Rouse*, 1977; *Bello and Smith*, 1990]. A lower mean α_{PT} value of 0.8 was derived for the period with available soil moisture in 1999. The same value of the α_{PT} was found by *Friedrich* [2001] at this location in an energy and water balance study in 1999. Similar values for α_{PT} were estimated for a well-drained upland lichen-heath tundra near Churchill, Manitoba (*Eaton et al.* [2001]: $\alpha_{PT} = 0.81$), and for dry upland regions characterized by sedge tussocks, mosses, and lichens (*Rouse and Stewart* [1972]: $\alpha_{PT} = 0.95$; *Stewart and Rouse*, [1976]: $\alpha_{PT} = 1.0$).

[14] The ground heat flux Q_g was calculated as change of soil sensible energy H_{gs} and soil latent energy H_{gl} per unit time using hourly time steps, $Q_g = \Delta(H_{gs} + H_{gl})$. The thermal energy stored as sensible heat at time t in the soil to a depth of 0.7 m (late summer season thaw depth and also maximum depth of TDR measurements) was estimated by summing the thermal energy of the soil components ice, i, liquid water, w, and soil matrix, sm, in the soil profile [*Boike et al.*, 1998]:

$$H_{gs} = \sum_{\alpha \in i,w,sm} c_\alpha \rho_\alpha \int \theta_\alpha(z,t)T(z,t)dz \qquad (3)$$

where c_α, is the specific heat capacity, ρ_α is the mass density, and θ_α, is the volumetric content of phase α, and T is the temperature. The latent heat energy of the soil was calculated as:

$$H_{gl} = -L_f \rho_i \int \theta_i(z,t)\ dz \qquad (4)$$

where $L_f = 0.333 * 10^6$ J kg^{-1} is the latent heat of fusion, ρ_i is the ice mass density, and θ_i is the volumetric ice content, which is estimated from TDR measurements of soil water content directly before the freeze-back of soils [*Boike et al.*, 1998]. This implicitly assumes that no significant lateral moisture redistribution takes place during winter. The reference state for the energy storage calculations is liquid water at 0°C.

[15] Due to technical problems in 1999, the soil volumetric water content necessary for calculation of H_{gl} is not available for the whole summer. Therefore the ground heat flux was calculated from temperature difference at depths z, using the thermal conduction equation [*Incropera and Dewitt*, 1996]:

$$Q_g = -\lambda \frac{\Delta T}{\Delta z}. \qquad (5)$$

[16] A constant soil thermal conductivity of $\lambda = 0.4$ W m^{-1} K^{-1} was applied. This value was obtained by linear best fit ($R^2 = 0.95$) of Q_g data from heat flux plate measurements and the thermal gradient calculated from temperature sensors located at 6 and 9 cm depth in 1998 [*Friedrich*, 2001]. The same value of λ was found using the thermal gradient and modeled $\Delta(H_{gs} + H_{gl})$ data when soil water content measurements were available in 1999. A comparable value for the effective thermal conductivity of surface organic soils of 0.3 W m^{-1} K^{-1} was found by *Hinzman et al.* [1991] in the study of hydrologic and thermal properties of soil in the Alaskan Arctic. A comparison of hourly estimates of heat fluxes using equations (3) and (4) and equation (5) for the period with available soil water content data in 1999 showed a good agreement between the two methods when the empirically derived
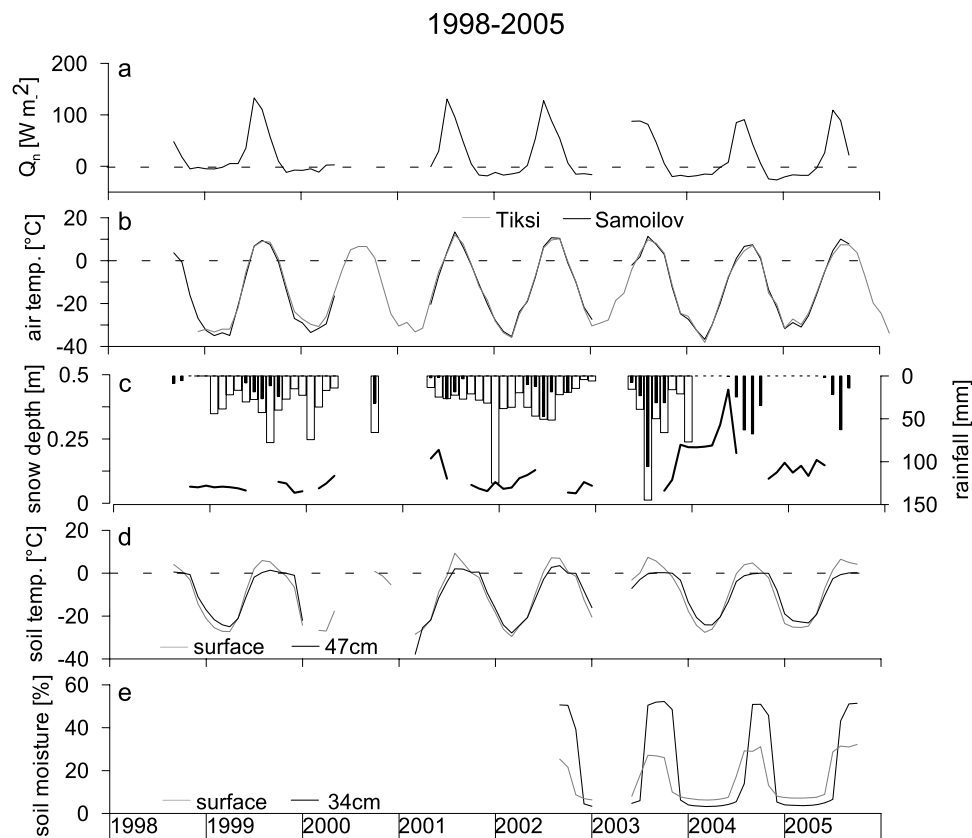
Figure 3. Monthly average meteorological and soil data from the monitoring station on Samoylov Island. (a) Net radiation; (b) air temperature for Samoylov (black) and Tiksi (grey); (c) snow depth and daily totals of rainfall for Samoylov (black filled bars) and Tiksi (non filled bars); (d) soil temperature at 47 cm depth and close to the surface (9 cm depth until July 2002, 6 cm depth thereafter); and (e) soil volumetric water content at 34 cm depth and surface.

value of λ was applied ($R^2 = 0.85$ for 14–17 May; $R^2 = 0.79$ for 14–15 August).

3.3. Water Balance Calculation

[17] The change of (surface and subsurface) water storage ΔS can be expressed as

$$P - ET - R = \Delta S \qquad (6)$$

where P is precipitation, ET is evapotranspiration when water is lost to the atmosphere (negative ET) or condensation when water is gained from the atmosphere (positive ET), and R is lateral surface and subsurface water flow. If lateral water flow R is neglected, the water storage can be estimated as:

$$P - ET = \Delta S_{est}. \qquad (7)$$

No snowfall occurred during the summer periods of 1999 and 2003, thus accumulation or melt of snow is not included in the water balance.

4. Results

4.1. Climatology 1998–2005

[18] Monthly average air temperatures during summer showed large variation between the years 1998–2005

(Figure 3b). July and August were the warmest months; but the monthly average varied between 6.6°C (July 2004) and 13.4°C (July 2001). The coldest period was typically January–February with monthly averages of about −35°C. The monthly average net radiation was typically highest during June, decreased strongly during July–September, and was negative from October (Figure 3a). It was continuously negative for 5 months during the winters 1998–1999 and 1999–2000, for 6 months during the winter of 2001–2002, and for 7 months during the winters 2003–2004 and 2004–2005. During the summers of 2003 and 2004, the net radiation was considerably lower (~20%) than during the years 1999–2002, which was caused by a prevalence of cloudy weather conditions in 2003, and a late snowmelt in 2004.

[19] Snow started to accumulate in September in most years (Figure 3c). The pattern of snow accumulation was very variable, as was the depth of the snow cover. During the winter 1998–1999, the maximum monthly average snow depth was recorded in December (7 cm), during the winter 2003–2004 it was recorded in May (44 cm). The snow usually melted within 7–10 d; in years with thin snow cover the snow was gone by the end of May or first days of June (1999, 2002, 2003), otherwise at about the middle of June (2001, 2004, 2005). Redistribution of snow by wind and the polygonal microtopography resulted in a spatially highly variable depth of the snow cover. For instance in the
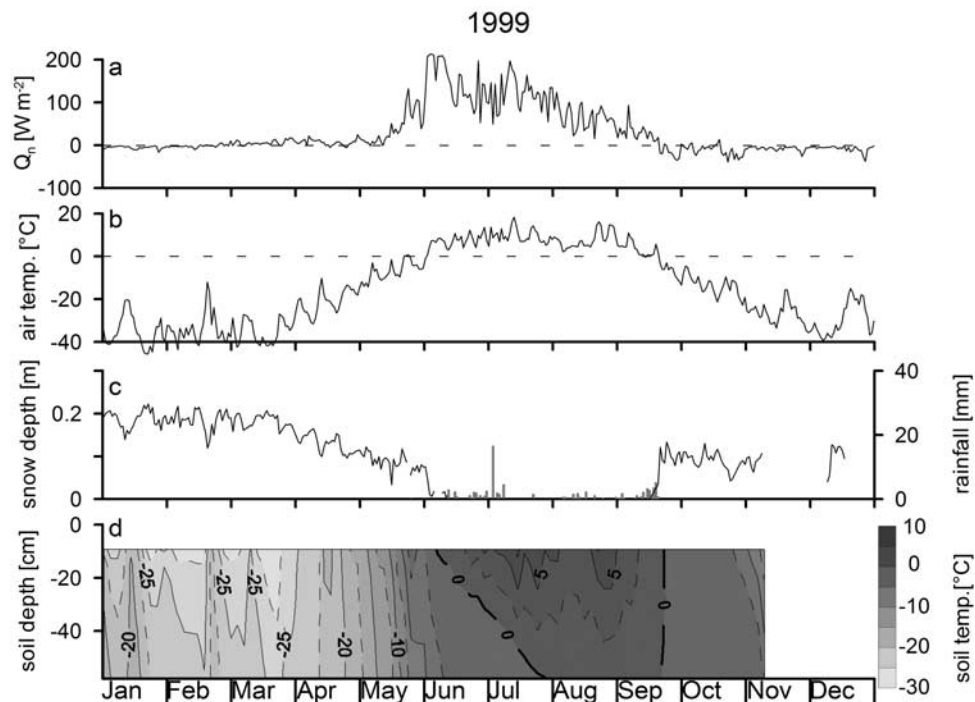
Figure 4. Daily average meteorological and soil data for 1999. (a) Net radiation, (b) air temperature at 2 m height, (c) snow depth and daily sums of rainfall (bar graph), and (d) soil temperature.

spring of 2004, snow depth varied between 40–50 cm in the polygon centers and 0–10 cm on the rims.

[20] Rainfall usually occurred between the middle of May and the middle of September, depending on the length of the frost period and the synoptic weather situation (Figure 3c). The total amount of rainfall measured varied between 72 and 88 mm in 2001 and 1999, and 193 and 208 mm in 2004 and 2003, respectively (mean 137 mm).

[21] Average monthly soil temperatures were generally low (Figure 3d). The maximum monthly temperature of the uppermost soil layer did not exceed 10°C; the maximum of 9.4°C was recorded in July 2001. The amplitude of seasonal surface temperature variations was 40 K (+10 to −30°C). Soil moisture in the thawed active layer for the years 2002–2005 showed only small differences between years (Figure 3e). In the organic surface layer, the average monthly water content reached about 20–30%, indicating that it was not saturated. This is expected since the elevated rim permits micro topographically controlled drainage of water. At a depth of 34 cm, the water content stayed close to 50% after thawing, which means that the sandy silt soil was always saturated. During winter, the liquid water content of the frozen soils was below 8%.

4.2. Meteorological and Soil Conditions 1999

[22] In the spring of 1999, the snow cover was thin with a depth of 20 cm in the polygon centers. The snow water equivalent before melt was about 40 mm. Snow thaw started around 25 May and lasted for about 10 d (Figure 4c). Before snowmelt, the snow exclusively sublimated, consuming about 50% of the available energy, and exposing the polygonal ridges [*Boike et al.*, 2003b]. Consequently, the net radiation reached large positive values already during snowmelt; it was on average 63 W m^{-2} during the second

half of May (Figure 4a). After snowmelt, net radiation increased strongly; it averaged to 145, 121, and 67 W m^{-2} in June, July, and August, respectively. The monthly average air temperature was 6.7, 9.7, and 7.8°C during June, July, and August, respectively (Figure 4b). There were only short warm periods which were associated with the advection of warm air from the south (14, 23 July, 23, 29 August); however, the first half of August was characterized by a pronounced cold period. The total rainfall for 1999 was 88 mm; for the period June–August it was 56 mm with highest intensity of about 3 mm h^{-1} on 4 July (Figure 4c).

[23] The soil thaw started at the beginning of June and progressed rapidly; the upper 9 cm of the soil profile were thawed by 10 June, the layer at 15 cm depth was thawed on 16 June (Figure 4d). On 24 July, the thaw front passed the lowest temperature sensor at 58 cm depth. From the increase of thaw depth during June and July, and the typical length of the soil thaw period (until early September), the maximum thaw depth was estimated to be at least 70 cm. The soil water content at 9 cm depth was 25% directly after thaw on 10 June, and 26% on 22 August. The water content at and below 15 cm depth (down to 0.47 cm) ranged from 42 to 49%, which indicates that the soil layers were close to saturation (data not shown). The freezing of the soil started during the second half of September and the ground remained isothermal (zero curtain) until mid October. The freezing front moved from the ground surface to the bottom of the active layer, and by 4 November the active layer was completely frozen.

4.3. Summer Energy and Water Balance 1999

[24] During June and July, the energy input of Q_n was 17–18 MJ m^{-2} d^{-1} on clear days and about 4 MJ m^{-2} d^{-1} on cloudy and rainy days such as 28 June and 4 July
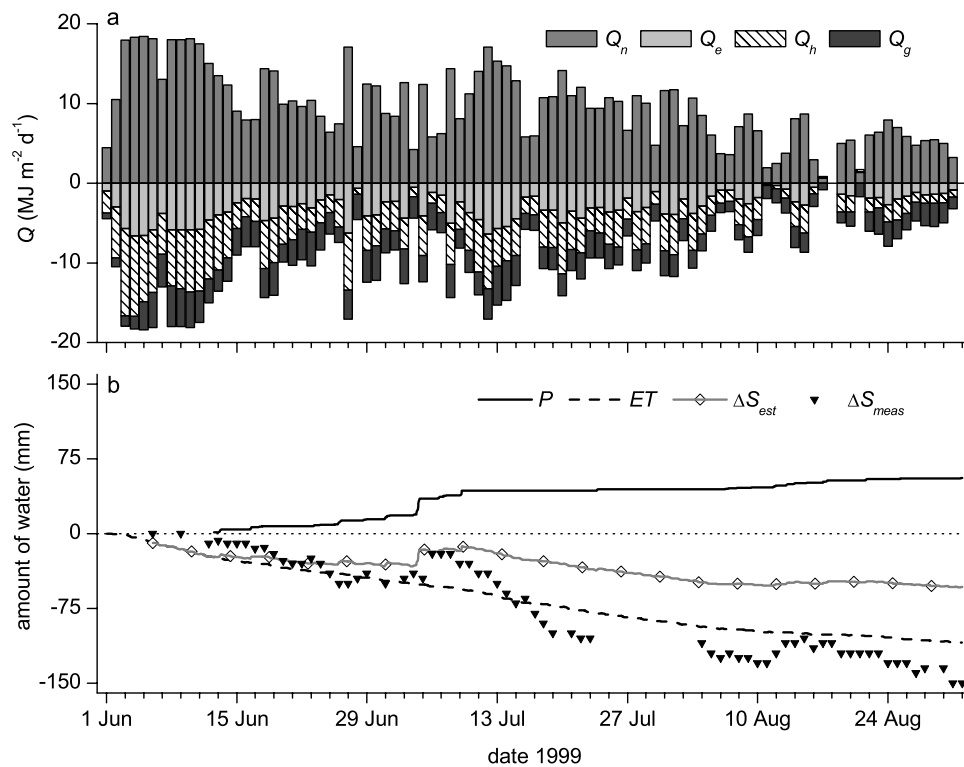
Figure 5. Energy and water balance components during the period 1 June to 31 August 1999. (a) Daily sums of energy balance components Q_n, Q_e, Q_h, and Q_g; (b) cumulative water balance components ΔS_{est} (equation (7)), and ΔS_{meas}.

(Figure 5a). The average energy input through Q_n was 12.5 MJ m^{-2} d^{-1} during June (1–13 June: 15.5 MJ m^{-2} d^{-1}), 10.3 MJ m^{-2} d^{-1} during July (14–31 July: 10.1 MJ m^{-2} d^{-1}), and 5.7 MJ m^{-2} d^{-1} during August. The energy input through rain Q_r was negligible on most days, the maximum value of 0.17 MJ m^{-2} d^{-1} was observed on 4 July (4% of Q_n). Q_h was the largest energy sink during June and July, consuming 43% (1–13 June: 48%) and 39% (14–31 July: 39%) of Q_n, respectively, and the second largest sink during August (35% of Q_n). Q_g was the smallest energy sink in June and July, consuming 26% (1–13 June: 20%) and 29% (14–31 July: 28%) of Q_n, respectively. However, during August, Q_g consumed 37% of Q_n and was the largest energy sink. Between 28 and 33% of Q_n went into Q_e, thus making it the second largest energy sink during June and July, and the smallest energy sink in August. Cumulative sums of all energy balance components over the complete summer period are given in Table 1.

[25] Over the course of the period June–August, the measured water storage ΔS_{meas} showed a generally decreas-ing trend; it was only markedly interrupted by the precipi-tation events on 4 July and 11–15 August (Figure 5b). Changes of ΔS_{est} and ΔS_{meas} were comparable until 8 July; afterward ΔS_{meas} decreased much faster than ΔS_{est}. Until 20 July, a difference of +70 mm built up between ΔS_{est} and ΔS_{meas}. After 20 July, the changes of ΔS_{meas} and ΔS_{est} were again similar; the difference between the two increased only slowly to +97 mm until 31 August (Table 2).

4.4. Meteorological and Soil Conditions 2003

[26] In 2003, due to technical problems there exist no data before 10 May and during the period 15 June to 12 July. The snow thaw started before 10 May and the snow was largely gone by 15 May (Figure 6c). However, due to cloudy weather conditions, the daily average net radiation seldom reached values >100 W m^{-2} until the middle of June; the average during the first half of June was 84 W m^{-2} (Figure 6a). Net radiation was also frequently low during July and August; the average values were 79 and 49 W m^{-2} for the period 14–31 July and during August, respectively. The average air temperature was 1.7, 11.2,

Table 1. Cumulative Energy Budget Components in 1999 and 2003[a]

	Q_n, MJ m^{-2}	Q_e, MJ m^{-2} (%)	Q_h, MJ m^{-2} (%)	Q_g, MJ m^{-2} (%)	Q_r, MJ m^{-2} (%)
1999	+866	−268	−345	−254	+0.58
1 Jun to 31 Aug		31	40	29	<0.1
1999	+353	−108	−131	−114	+0.05
14 Jul to 31 Aug		31	37	32	0.0
2003	+257	−158	−57	−52/+9	+0.36
14 Jul to 31 Aug		61	22	20/3	0.1

[a]Values are given as totals and in percent of Q_n.

Table 2. Water Balance Components for 1999 and 2003

	P, mm	ET, mm	ΔS_{est}, mm	ΔS_{meas}, mm
1999				
1 Jun to 31 Aug 1999	+56	−109	−53	−150
14 Jul to 31 Aug 2003	+13	−44	−31	−90
14 Jul to 31 Aug	+135	−63	+72	−10

and 7.7 C during 1–13 June, 14–31 July, and August, respectively (Figure 6b). Daily average air temperatures in the middle of July and at the beginning of August were frequently greater than 15°C (Figure 6b). These pronounced warm periods were separated by a cold period at the end of July which was accompanied by heavy rainfall (94 mm). During this event, large rainfall intensities between 6 and 7.7 mm h^{-1} were observed on 22 and 24 July. The total amount of rainfall during the period 14 July to 22 October was 168 mm (Figure 6c). The soil thaw started at the beginning of June, and the surface at 5 cm depth thawed between 7 and 12 June (Figure 6e). The progression of the thaw front was slower compared to 1999; on 24 July 2003 the thaw depth was between 37 and 47 cm (1999: 58 cm). Thus the thaw depth was at least 10 cm smaller in 2003 compared to 1999. Soil freeze back (zero curtain effect) started from the top of the profile on 30 September. The late

freeze back is due to advection of warm continental air from the south that led to unusually warm air temperatures at the beginning and during the second half of September. Freeze back was completed by 11 November, when the layer at 50 cm depth froze. At the beginning of July, the soil was water-saturated only below a depth of 12 cm (Figure 6d). During the large rainfall at the end of July, also the surface layer became saturated. However, after a few days the water content decreased and then remained about 20% below saturation until the freeze back of soils. The profile below this layer was saturated throughout the summer. The differences in soil moisture below 20 cm depth indicate soil texture differences. Of note is the steep step increase in soil moisture in thawed and frozen soil in July and August during and after the two rainfall events indicating the infiltration of water into frozen soil.
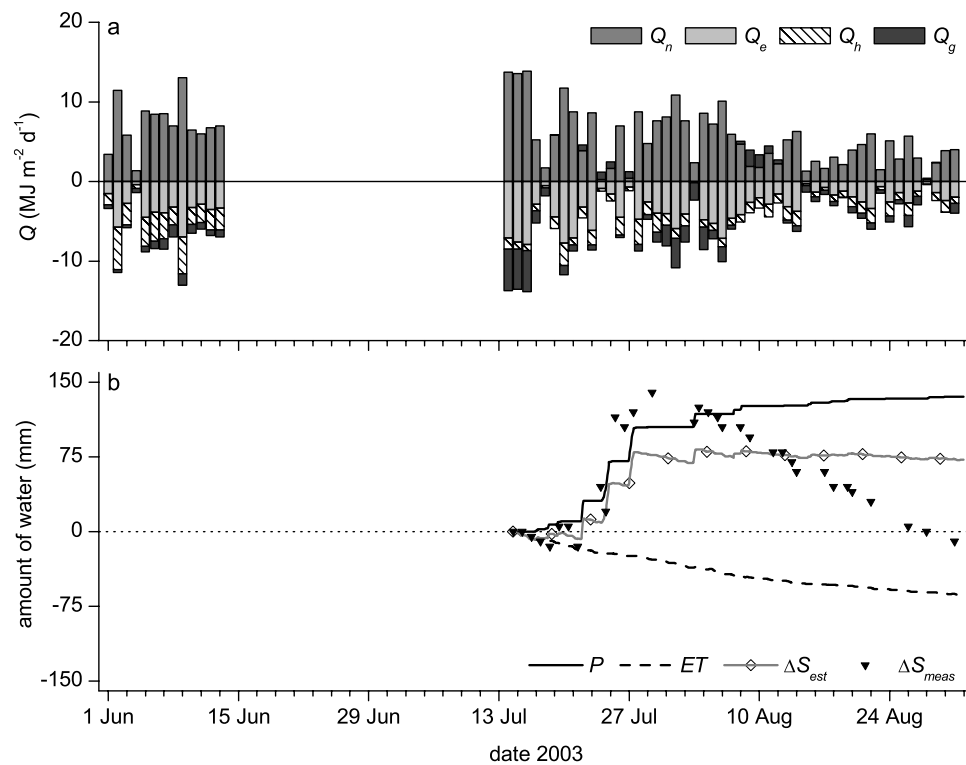
4.5. Summer Energy and Water Balance 2003

[27] The daily energy input through Q_n was on average 7.2, 7.0, and 4.3 MJ m^{-2} d^{-1} during 1–13 June, 14–31 July, and August, respectively. On the cloudy and rainy days 24 and 27 July, total Q_n was less than 0.5 MJ m^{-2} d^{-1} (Figure 7a). During these days, Q_r was significant; it was an energy source of 10% of Q_n on the relatively warm 24 July (mean air temperature +7.9°C), whereas it was an energy sink of 19% of Q_n on the relatively cold 27 July (+3.3°C). Q_e was the largest energy sink on most days. The percentage of Q_n
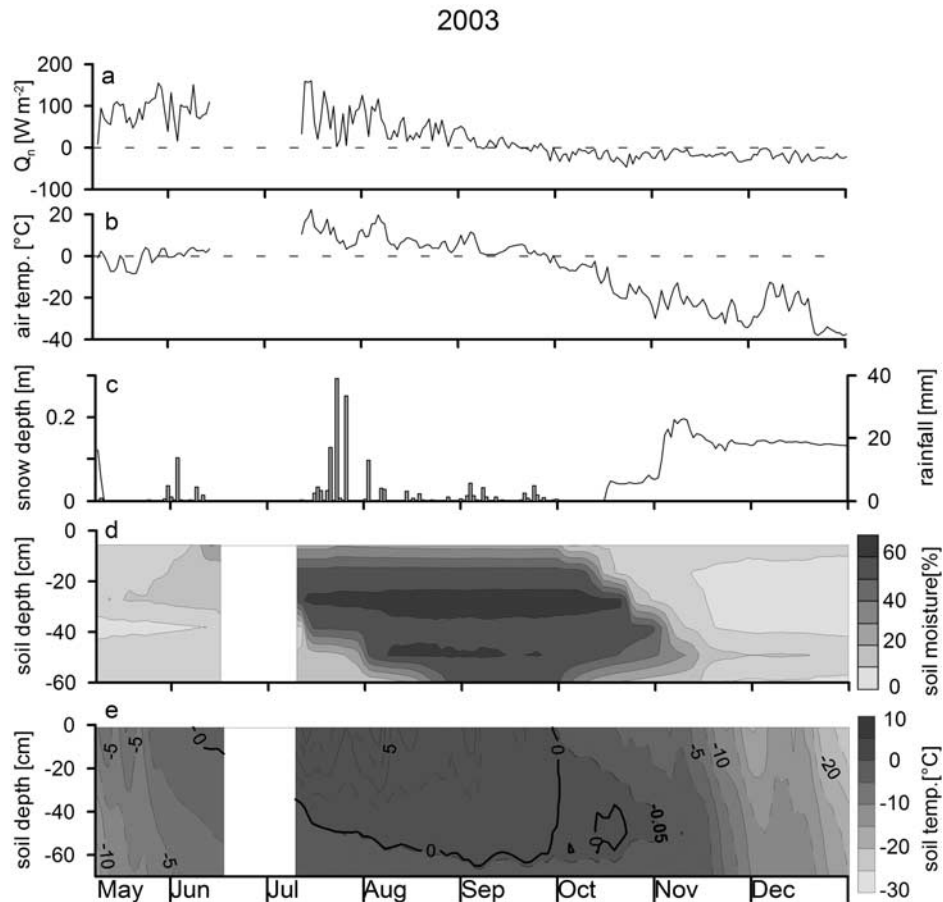
Figure 6. Daily average meteorological and soil data for 2003. (a) Net radiation, (b) air temperature at 2 m height, (c) snow depth and daily sums of rainfall (bar graph), (d) soil temperature, and (e) soil moisture. Because of technical problems there are no data before 10 May and during the period 15 June to 12 July.

Figure 7. Energy and water balance components in 2003. (a) Daily sums of energy balance components Q_n, Q_e, Q_h, and Q_g for the periods 1–13 June and 14 July to 31 August; (b) cumulative water balance components for the period 14 July to 31 August ΔS_{est} (equation (7)), and ΔS_{meas}.

which went into Q_e was 49% during 1–13 June, 62% during 14–31 July, and 61% during August. Q_h was the second largest energy sink; 39, 20, and 24% of Q_n went into Q_h during 1–13 June, 14–31 July, and August, respectively. Q_g consumed 12% of Q_n during 1–13 June, 18% during 14–31 July, and 15% during August, and was the smallest energy sink. During cold and cloudy days, e.g., 22–27 July and 8–12 August, the ground was a source of energy and returned about one seventh of the gross Q_g to the atmosphere. Of the remaining energy, 98% went into the change of soil latent heat, i.e., the thaw of the ice rich permafrost soil.

[28] The water storage in 2003 was characterized by the repeated strong rain events at the end of July (Figure 7b). However, ΔS_{meas} and ΔS_{est} reacted markedly different: During the period 21–29 July ΔS_{meas} increased by 155 mm, whereas ΔS_{est} increased by only 70 mm. Also after the rain events, ΔS_{meas} and ΔS_{est} behaved differently: Until 31 August, ΔS_{meas} decreased continuously by roughly 5 mm d^{-1} while ΔS_{est} decreased by only 5 mm, because ET and R nearly balanced. Thus the difference between ΔS_{est} and ΔS_{meas} changed from −63 mm on 29 July to +82 mm on 31 August (Table 2).

4.6. Comparison of Water Balance 1999 and 2003

[29] For quantitative analyses of the water balance, ΔS_{est} and ΔS_{meas} were plotted against each other for several periods with low precipitation (Figure 8). As indicated by the slope of the linear regressions, in 1999 measured storage decreased 4 and 7 times faster than estimated storage, whereas in 2003, measured storage decreased about 20 times

faster. This indicates that ΔS_{est}, which is based on P-ET and excludes lateral surface and subsurface flows, does not describe the water balance of the polygonal tundra adequately. In 2003 during and after strong rain events, surface runoff and channel formation was observed. In 1999, no visible surface flow into or out of ponds was observed because the water level position was already below the soil surface in the polygon center.

4.7. Subsurface Flow Experiment

[30] A dye tracer experiment was undertaken in August 2006 to evaluate the flow of water between polygons through the polygonal rim (Figure 9). On 21 August 10 L of water dyed with a blue tracer (5 mg L^{-1} Vitasyn Blue AE85, Hoechst AG, Germany) were poured in a pit (45 cm × 15 cm wide) which had been dug to the thaw depth of 30 cm. The pit was located at the outermost edge of the polygonal rim separating polygon A and B (Figures 9a and 9b). The location for the experiment was chosen at a rim that was not divided by a crack since only subsurface flow (and not surface flow inside the crack) was the scope of this study. The difference in water level between Polygons A and B was 5 cm. It was hypothesized that subsurface water flowed between these two polygons. On 30 August further pits were dug to visualize the subsurface pathways of the tracer dye. Within 9 d, blue water had moved 1.3 m toward polygon B within a 3–5 cm layer of fine to medium sand. This sand layer was bounded by lower hydraulic conductivity layers (sandy silt) above and below (Figure 9c). Using Darcy's law [*Freeze and Cherry*, 1979] and a hydraulic conductivity of 1.30×10^{-4} m s^{-1} for a 5 cm sand layer (estimated from the
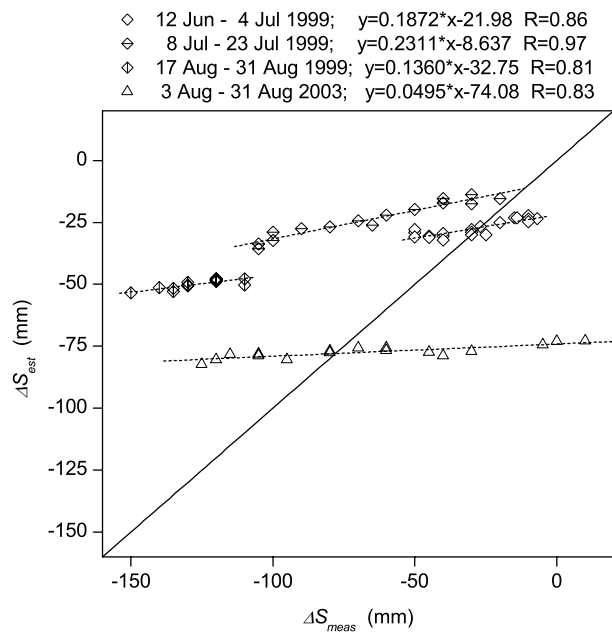
Figure 8. Estimated storage (cumulative *P-ET*) versus measured storage during periods with low precipitation in 1999 and 2003. For 2003 data the sign was reversed for better illustration. The dashed lines are linear fits of the data, the solid line is the function y = x.

tracer experiment), a distance of 4 m between polygons (width of polygon rim), an estimated polygon pond surface area of 100 m^2, and a time 60 d (July–August), the total water transported via groundwater flow would result in a water level decrease of 42 mm in polygon A. This values lies in the same order of magnitude of difference between estimated and measured storage change in 1999 (59 mm).

4.8. Seasonal Drivers of Energy Balance

[31] The relationship of energy partitioning and air temperature was illustrated by comparison of the ratio of Q_e, Q_h, Q_g, and Q_n for different air temperature ranges (Figure 10). In both years 1999 and 2003, Q_e/Q_n increased and Q_h/Q_n decreased with increasing air temperature. However, the sensitivity of Q_e/Q_n to air temperature was more pronounced during the wet year 2003 compared to the dry year 1999: Qe/Qn increased by 21% in 2003 and by only 7% in 1999 between the temperature classes <0°C and >15°C, With an increase of 34% between temperature classes <0°C and >15°C during both years, the sensitivity of Q_h/Q_n to air temperature was greater than that of Q_e/Q_n, but did not depend on the moisture regime.

5. Discussion

5.1. Summer Energy Balance 1999 and 2003

[32] The total Q_n during June to August 1999 of 868 MJ m^{-2} is very similar to the value of 854 MJ m^{-2} reported by *Ohmura* [1982] for a tundra site at Barrow, Alaska (71°N), and the values of 700–800 MJ m^{-2} reported by *Lloyd et al.* [2001] from Zackenberg, Greenland (74°N) and Skalluvaara,
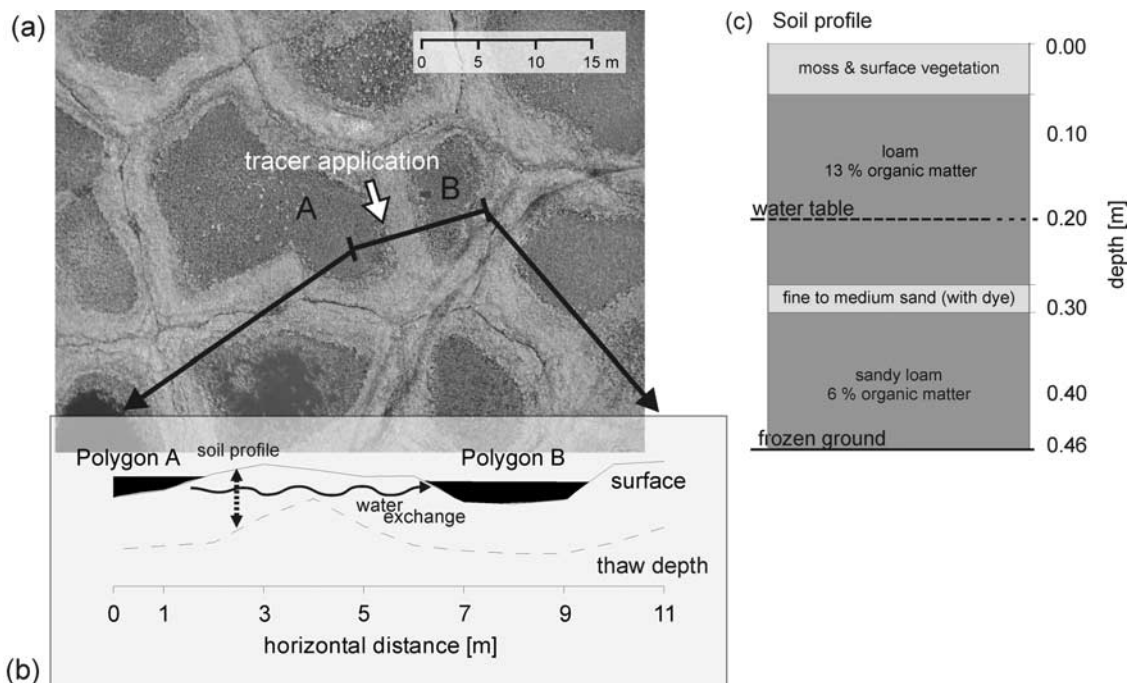
Figure 9. Scheme of subsurface flow tracer experiment in August 2006. (a) Aerial picture of experimental site, (b) cross section A-B, the width of the polygonal wall was about 4 m and the thaw depth at the soil profile where the dye tracer was applied was 46 cm, and (c) typical soil profile along A-B at the end of the experiment. The dye was exclusively found in a continuous sand layer, approximately 3 cm thick.
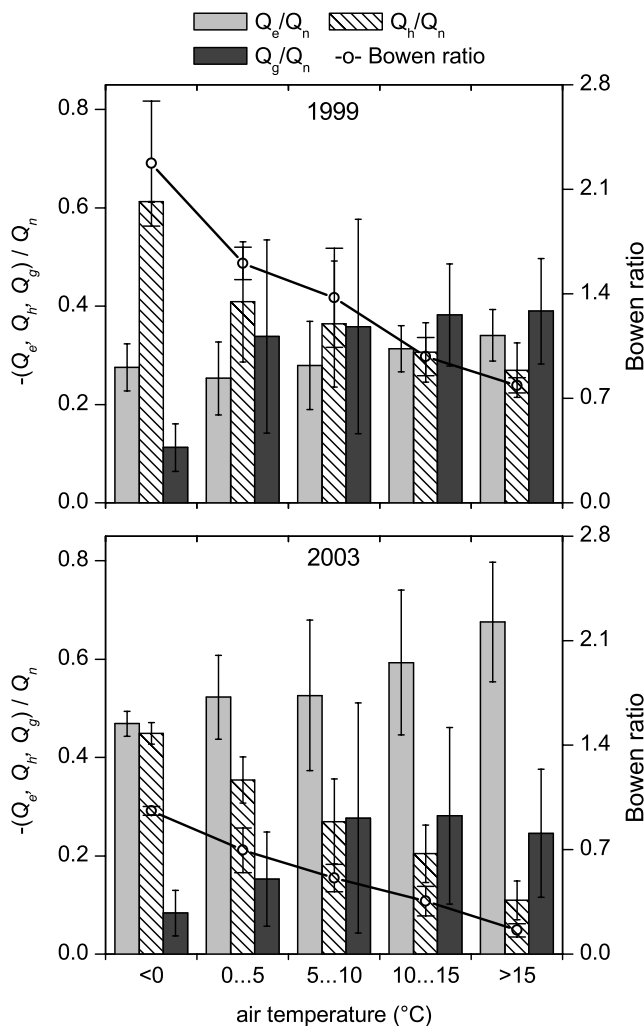
Figure 10. Bowen ratio and ratios of energy fluxes Q_e, Q_h, Q_g, and net radiation Q_n based on daily sums of fluxes as displayed in Figures 5 and 7. The data were grouped into five bins according to mean daily air temperature and averaged within each bin. The error bars are standard deviations within the bins. During days with positive Q_g in 2003, Q_g/Q_n was disregarded and $Q_e/(Q_n + Q_g)$ and $Q_h/(Q_n + Q_g)$ was used.

Finland (70°N) for the period 9 June to 29 August. However, Q_n differed greatly between the years 1999 and 2003. During the period 14 July to 31 August, the available energy was 24% lower in 2003 compared to 1999. This was due to the predominance of cloudy weather in 2003, which is exemplified by the cloudy and rainy period at the end of July when Q_n was reduced to less than 10% of the monthly average.

[33] The fraction of 29% of Q_n that was partitioned into Q_g in 1999 was large compared to values of Q_g/Q_n of 10–16% reported from North American [*Ohmura*, 1982; *Vourlitis and Oechel*, 1997; *Harazono et al.*, 1998] and European Arctic sites [*Harding and Lloyd*, 1998; *Soegaard et al.*, 2001]. In general, the Q_g/Q_n ratio is low for wetlands due to the high soil moisture content and a high evapotranspiration [*Jacobsen and Hansen*, 1999]. The high soil heat flux at our site in 1999 is explained by the generally dry soil

conditions which, compared to wet tundra soils, led to lower soil hydraulic conductivity and thus less evaporation [*Boike et al.*, 1998] and hence an overall shift of the energy partitioning toward Q_g. This is supported by the increase of the value of Q_g/Q_n from 26% in June to 37% in August 1999, which concurs with a falling water table and further drying of the upper soil layers. On the other hand, the Q_g/Q_n value of 17% found in 2003 is closer to the results of the studies cited above, albeit at the upper end of the range given there. This could be explained by the low permafrost temperature in our study region, which leads to a strong temperature gradient in the thawed soil layer and promotes a generally high ground heat flux during summer [*Boike et al.*, 2003b].

[34] The fractions of Q_n that were partitioned into Q_e (61%) and Q_h (22%) in 2003 are comparable to values found by other arctic wetland studies. Values of Q_e/Q_n and Q_h/Q_n reported are 57% and 29% for a flooded sedge tundra at the North Slope of Alaska [*Harazono et al.*, 1998], 39% and 27% for an Arctic fen at northeast Greenland [*Soegaard et al.*, 2001], 64% and 28% for two Canadian sub-Arctic tundra sites [*Eaton et al.*, 2001], and 51% and 34% for a sub-Arctic elevated mire in Northern Finland [*Lloyd et al.*, 2001]. The mean Bowen ratio, β, for the measurement periods 2003 was 0.36. Thus in 2003 the tundra behaved like a typical wetland in terms of the energy partitioning. In 1999, the energy partitioning was drastically different compared to 2003. The fractions of Q_n that were partitioned into Q_e and Q_h were 31% and 40%, respectively, and the mean Bowen ratio was 1.29. The smaller value of Q_e/Q_n was caused by the drying of the upper soil and the moss layer. It is thought that a substantial part of 50–85% of tundra ET is evaporation from the moss layer [*Miller et al.*, 1980; *Vourlitis and Oechel*, 1999; *Grant et al.*, 2003]. Mosses lack stomatal control, but their resistance to water loss was shown to increase exponentially as tissue water decreases [*Oechel and Sveinbjörnsson*, 1978; *McFadden et al.*, 2003].

[35] During both years, the Bowen ratio was largest in June (1999: 1.39; 2003: 0.81), was lowest in July (1.19/ 0.32), and rose again slightly in August (1.24/0.40). A similar pattern was observed at Arctic and boreal wetlands in Europe, North America, and Greenland [e.g., *Lafleur et al.*, 1997; *Lloyd et al.*, 2001]. It can be explained by the phenological development of vascular plants in the tundra canopy and their contribution to the total tundra ET and hence Q_e. The fact that the seasonal change of the Bowen ratio was observed during both years 1999 and 2003 suggests that despite the dry conditions and the low water level in 1999, vascular plants were not limited by water availability. This is supported by the typical root horizon depth of 11–26 cm in polygon centers and 0–15 cm at polygon rims [*Kutzbach et al.*, 2004], and the soil moisture measurements which showed that soils were close to water saturation at all times at and below depths of 15 cm.

5.2. Seasonal Drivers of Energy Balance

[36] Net radiation was the dominant energy source, as visualized in Figures 5a and 7a. However, the large variations in daily Bowen ratio indicate that the turbulent fluxes of energy are driven not by net radiation alone. *Harazono et*
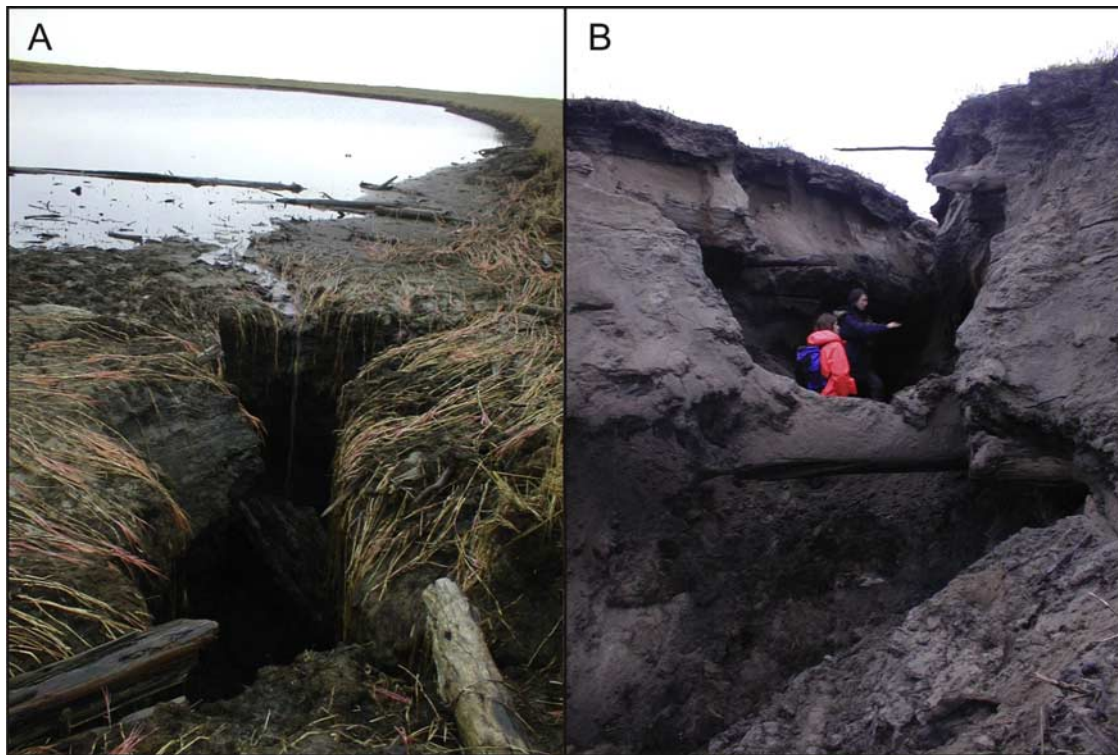
Figure 11. Thermoerosion features at the polygonal tundra of Samoylov Island, initiated by strong rainfall events in summer 2003. (A) A large lake is drained by one outflow. The log at the front right has a length of about 1 m. (B) Drainage channel outflow at the cliff of the river terrace that builds up the Eastern part of Samoylov Island [from *Kutzbach*, 2006].

al. [1998] related observed fluctuations of Bowen ratio at a wet sedge tundra at the North Slope, Alaska to air temperature variations connected to synoptical weather patterns, namely the change between onshore winds from the Arctic Ocean and offshore winds from the continental hinterland. This finding is thought to apply also to our study site. During periods of advection of continental warm and dry air masses (e.g., 14–16 July 2003), Q_g/Q_n was greatly increased (37%) and Q_h/Q_n was very low (7%). On the other hand, during periods of advection of maritime cold air (e.g., 24–27 July 2003), the soil turned into a significant source of heat (25% of Q_n), and Q_h increased greatly (42%).

[37] The strong decline of Q_h/Q_n with increase in air temperatures (Figure 10) is the result of the reduction in surface to air temperature gradients and demonstrates the importance of air temperature as a driver of Q_h. The ratio Q_g/Q_n increased initially with increasing temperature but shows no further increase in the temperature range above 10°C during both years 1999 and 2003. This could be explained by the increased thaw depth, which reduces the temperature gradient and thus leads to a reduction of Q_g. All the above findings are in agreement with the results by *Harazono et al.* [1998], who compared the relationship of energy partitioning and air temperature of a wet sedge tundra and a dry tussock tundra at the North Slope of Alaska during one growing season.

[38] In summary, the air temperature has a significant influence on the energy partitioning of the tundra. Because of the location of the study site at the border between continental and maritime arctic air masses, the synoptical

weather patterns are of major importance for the energy balance of the tundra.

5.3. Comparison of Water Balance 1999 and 2003

[39] The evaluation of the water balance of the polygonal pond demonstrated the response of water balance components to climatic variability between two study seasons. In 2003, high precipitation inputs resulted in the recharge of polygonal ponds. Similarly, *Woo and Guan* [2006] found that arctic ponds can be recharged to snowmelt levels by sizable rain events. *Bowling et al.* [2003] showed that late summer precipitation may result in runoff from upland tundra areas to partially recharge pond storage. On the other hand, low amounts of precipitation in 1999 resulted in a total loss of pond surface waters. This underlines the importance of the frequency and duration of precipitation events in the water budget of polygonal ponds during the postsnowmelt season. *Kane and Carlson* [1973] concluded from their studies that direct precipitation was the major hydrologic input to an arctic lake in the Low Arctic.

[40] Evapotranspiration led to a steady pond storage decline in both study seasons. Even during the dry year of 1999 evaporation continued during the whole summer, despite the fact that water levels fell well below the soil surface in the depressed polygon centers. This is explained by the large depth of 34 cm of the rooting zone in the polygonal centers [*Kutzbach et al.*, 2004], which guaranteed the availability of water for plant uptake. According to *Lafleur et al.* [2005], the rooting depth of vascular plants represents a critical limit of water table depth, below which

evapotranspiration is limited to some degree by water supply.

[41] However, water balance calculations based on P-ET did not describe the water balance of the polygonal tundra adequately (Figures 5 and 7). The storage loss in 1999 must have been due to subsurface outflow of water. The trace experiment conducted in August 2006 suggests a possible connection of the pond with neighboring ponds via subsurface flow through sandy soil layers with high hydraulic conductivity. The occurrence of sand layers is widespread as found in detailed cross sections of low centered polygons on Samoylov Island [*Pfeiffer et al.*, 2002]. The occurrence of thin sandy layers with higher hydraulic conductivity compared to the prevalent loam or silt layers could also explain the varying speed of the storage loss in 1999. *Woo and Guan* [2006] found during a post snowmeltwater balance study of tundra ponds that, in addition to vertical fluxes, change in the pond storage was driven by low magnitude lateral flow exchanges with neighboring ponds. The importance of lateral fluxes for the seasonal water balance of a northern boreal fen during a dry year was also shown by *Lafleur et al.* [1997], who observed that the fen drained gradually throughout the summer in response to evaporation and lateral outflow. Furthermore, a subsurface hydrologic connections enable the transport of nutrients which could be an important factor for sustaining this wetland ecosystem.

[42] In 2003, high soil moisture conditions and a high water table together with a shallow active layer contributed to surface connectivity of the pond with the surrounding catchment during and after rain events. Field observations during the 2003 rain event included runoff across polygon rims and the development and widening of old and new hydrologic channels due to thermo-erosion (Figure 11). This surface runoff was the reason for the much larger decrease of ΔS_{meas} compared to ΔS_{est} as illustrated in Figure 8. Similarly, during the strong rain events in 2003, ΔS_{meas} increased much stronger than ΔS_{est} which suggests the inflow of water. *Woo and Guan* [2006] observed at their polygonal tundra pond research site in the Canadian Arctic that, during high and prolonged rain events, surface connectivity between the ponds was established through lateral surface flow, which recharged the ponds. They also suggest that cracks may act as natural channels for pond drainage. The formation of new channels as observed at our study site in 2003 was important for the regulation of surface runoff during extensive rain events, and may have a strong and lasting effect on the hydrologic connectivity within this tundra system.

[43] For both years, water balance calculations based solely on P-ET calculations underestimated the water budget of this polygonal tundra due to omission of surface and subsurface flows.

6. Conclusion

[44] The summer water balance of the studied wetland tundra was found to be mainly controlled by precipitation. Furthermore, the partitioning of the available energy was controlled by precipitation via the moisture regime of the tundra soils. The two years showed very different regimes in terms of the energy partitioning and it's relation to air temperature. During the dry year, the available energy was largely evenly partitioned between Q_e, Q_h, and Q_g for all air temperatures >0°C. During the wet year, the flux partitioning was highly dependent on air temperature: Q_e increased strongly with air temperature and drastically reduced the energy available for Q_h and Q_g. Hence with increasing air temperature and abundant moisture supply as predicted by global climate scenarios [*IPCC*, 2001], evaporation could increase strongly, thus reducing the sensible and ground heat flux.

[45] The formation of new surface flow channels through thermo-erosion and the drainage is expected to have a strong and lasting influence on the hydrologic system of the tundra. Subsurface flow is important in the tundra water budget, which is shown by gross underestimation of the water budget calculated from P-ET alone. These processes are not well understood and require further experimental and modeling studies. Improving our understanding of land atmosphere exchange processes will allow evaluating the degree of sensitivity of heat and water budget components to climate change in these northern permafrost landscapes.

Notation

Q_n	net radiation balance
Q_h	turbulent fluxes of sensible heat
Q_e	turbulent fluxes of latent heat
Q_r	heat flux supplied by rain
Q_g	ground heat flux
H_{gl}	thermal energy stored as latent heat in the soil
H_{gs}	thermal energy stored as sensible heat in the soil
α_{PT}	empirical parameter expressing actual to equilibrium evapotranspiration
α	phase (ice, i, liquid water, w, soil matrix, sm)
c_α	specific heat capacity
ρ_α	mass density
θ_α	volumetric content of phase α
T	temperature
z	depth
λ	soil thermal conductivity
P	precipitation
ET	evapotranspiration
S	surface storage
R	surface discharge
γ	psychrometric constant

References

Bello, R., and J. D. Smith (1990), The effect of weather variability on the energy balance of a lake in the Hudson Bay Lowlands, Canada, *Arct. Alp. Res.*, 22(1), 98–107.

Berezovskaya, S., D. Yang, and D. Kane (2004), Compatibility analysis of precipitation and runoff trends over the large Siberian watersheds, *Geophys. Res. Lett.*, 31, L21502, doi:10.1029/2004GL021277.

Berezovskaya, S., D. Yang, and L. Hinzman (2005), Long-term annual water balance analysis of the Lena river, *Global Planet. Change*, 48, 84–95.

Boike, J., and K. Roth (1997), Time domain reflectometry as a field method for measuring water content and soil water electrical conductivity at a continuous permafrost site, *Permafrost Perigl. Process.*, 8, 359–370.

Boike, J., K. Roth, and P. P. Overduin (1998), Thermal and hydrologic dynamics of the active layer at a continuous permafrost site (Taymyr Peninsula, Siberia), *Water Resour. Res.*, *34*, 355–363.

Boike, J., K. Roth, and O. Ippisch (2003a), Seasonal snow cover on frozen ground: Energy balance calculations of a permafrost site near Ny-Ålesund, Spitsbergen, *J. Geophys. Res.*, *108*(D2), 8163, doi:10.1029/2001JD000939.

Boike, J., L. D. Hinzman, P. P. Overduin, V. Romanovsky, O. Ippisch, and K. Roth (2003b), A comparison of snow melt at three circumpolar sites: Spitsbergen, Siberia, Alaska, in *Permafrost: Proceedings of the 8th International Conference on Permafrost 2003*, edited by L. U. Arenson, M. Phillips, and S. M. Springman, pp. 79–84, Balkema Publishers, Netherlands.

Bowling, L. C., D. L. Kane, R. E. Gieck, L. D. Hinzman, and D. P. Lettenmaier (2003), The role of surface storage in a low-gradient arctic watershed, *Water Resour. Res.*, *39*(4), 1087, doi:10.1029/2002WR001466.

Campbell, G. S. (Ed.) (1985), *Soil Physics With BASIC: Transport Models for Soil-Plant Systems*, 150 pp., Elsevier, New York.

Chapin, F. S., III, et al. (2000), Arctic and boreal ecosystems of western North America as components of the climate system, *Global Change Biol.*, *6*, 211–223.

Eaton, A. K., W. R. Rouse, P. M. Lafleur, P. Marsh, and P. D. Blanken (2001), Surface energy balance of the western and central Canadian subarctic: Variations in the energy balance among five major terrain types, *J. Clim.*, *14*, 3692–3703.

Eichinger, W., M. B. Parlange, and H. Stricher (1996), On the concept of equilibrium evaporation and the value of Priestley-Taylor coefficient, *Water Resour. Res.*, *32*, 161–164.

Eugster, W., et al. (2000), Land-atmosphere energy exchange in Arctic tundra and boreal forest: Available data and feedbacks to climate, *Global Change Biol.*, *6*(Suppl. 1), 84–115.

Fiedler, S., D. Wagner, L. Kutzbach, and E.-M. Pfeiffer (2004), Element redistribution along hydraulic and redox gradients of low-centered polygons, Lena Delta, Northern Siberia, *Soil Sci. Soc. Am. J.*, *68*, 1002–1011.

Freeze, R. A., and J. A. Cherry (1979), *Groundwater*, 604 pp., Prentice-Hall, Englewood Cliffs, N. J.

Friedrich, K. (2001), Energie-und Wasserhaushalt eines Tundrenstandortes im Lena-Delta, Diploma thesis, 74 pp., Tech. Univ. Dresden, Inst. for Hydrol. and Meteorol., Dresden, Germany.

Gilg, O., R. Sané, D. V. Solovieva, V. I. Pozdnyakov, B. Sabard, D. Tsanos, C. Zöckler, E. G. Lappo, E. E. Syroechkovski Jr., and G. Eichhorn (2000), Birds and mammals of the Lena Delta nature reserve, Siberia, *Arctic*, *53*(2), 118–133.

Grant, R. F., W. C. Oechel, and C.-L. Ping (2003), Modelling carbon balances of coastal tundra under changing climate, *Global Change Biol.*, *9*(1), 16–36, doi:10.1046/j.1365-2486.2003.00549.x.

Harazono, Y., M. Yoshimoto, M. Mano, G. L. Vourlites, and W. C. Oechel (1998), Characteristics of energy and water budgets over wet sedge and tussock tundra ecosystems at North Slope in Alaska, *Hydrol. Proc.*, *12*, 2163–2183.

Harding, R. J., and C. R. Lloyd (1998), Fluxes of water and energy from three high latitude tundra sites in Svalbard, *Nord. Hydrol.*, *29*(4/5), 267–284.

Hinzman, L. D., D. L. Kane, R. E. Giek, and K. Everett (1991), Hydrologic and thermal properties of the active layer in the Alaskan Arctic, *Cold Reg. Sci. Technol.*, *19*, 95–110.

Hinzman, L. D., D. J. Goering, and D. L. Kane (1998), A distributed thermal model for calculating soil temperature profiles and depth of thaw in permafrost regions, *J. Geophys. Res.*, *102*, 28,975–28,911.

Incropera, F. P., and D. P. Dewitt (1996), *Fundamentals of Heat and Mass Transfer*, John Wiley, New York.

IPCC (2001), Climate Change 2001: Impacts, Adaptation, and Vulnerability, in *Contribution of Working Group II to the Third Assessment Report of the Intergovernmental Panel on Climate Change*, Cambridge Univ. Press, Cambridge, U.K.

Jacobsen, A., and B. U. Hansen (1999), Estimation of soil heat flux/net radiation ratio based on spectral vegetation indexes in high-latitude Arctic areas, *Int. J. Remote Sens.*, *20*(2), 445–461.

Kane, D. L., and R. E. Carlson (1973), Hydrology of the central arctic river basins of Alaska, *Report, IWR-41*, 51 pp., Inst. of Water Resour., Univ. of Alaska, Alaska.

Kotlyakov, V., and T. Khromova (2002), Permafrost, Snow and Ice, in *Land Resources of Russia* [CD-ROM], edited by V. Stolbovoi and I. McCallum, Int. Inst. of Appl. Syst. Analysis and the Russian Academy of Science, Laxenburg, Austria.

Kutzbach, L. (2006), The Exchange of Energy, Water and Carbon Dioxide between Wet Arctic Tundra and the Atmosphere at the Lena River Delta, Northern Siberia, in *Reports on Polar and Marine Research 541*, 157 pp., Alfred Wegener Institute, Bremerhaven, Germany.

Kutzbach, L., D. Wagner, and E.-M. Pfeiffer (2004), Effect of microrelief and vegetation on methane emission from wet polygonal tundra, Lena Delta, Northern Siberia, *Biogeochemistry*, *69*, 341–362.

Lafleur, P. M., J. H. McCaughey, D. W. Joiner, P. A. Bartlett, and D. E. Jelinski (1997), Seasonal trends in energy, water, and carbon dioxide fluxes at a northern boreal wetland, *J. Geophys. Res.*, *102*, 29,009–29,020.

Lafleur, P. M., R. A. Hember, W. A. Stuart, and N. T. Roulet (2005), Annual and seasonal variability in Evapotranspiration and water table at a shrub-covered bog in southern Ontario, Canada, *Hydrol. Process.*, *19*(18), 3533–3550.

Lloyd, C. R., R. J. Harding, T. Friborg, and M. Aurela (2001), Surface fluxes of heat and water vapour from sites in the European Arctic, *Theor. Appl. Climatol.*, *70*, 19–33.

Lynch, A. H., F. S. Chapin III, L. D. Hinzman, W. Wu, E. Lilly, G. Vourlitis, and E. Kim (1999), Surface energy balance on the Arctic tundra: Measurements and models, *J. Clim.*, *12*, 2585–2606.

Marsh, P., W. R. Rouse, and M. Woo (1981), Evaporation at a High Arctic site, *J. Appl. Meteorol.*, *20*, 713–716.

McFadden, J. P., and W. Eugster (2003), A regional study of the controls on water vapour and CO_2 exchange in arctic tundra, *Ecology*, *84*(10), 2762–2776.

Mendez, J., L. D. Hinzman, and D. L. Kane (1998), Evapotranspiration from a wetland complex on the Arctic coastal plain of Alaska, *Nord. Hydrol.*, *29*, 303–330.

Miller, P. C., P. J. Webber, W. C. Oechel, and L. L. Tieszen (1980), Biophysical processes and primary production, in *An Arctic Ecosystem: The Coastal Tundra at Barrow, Alaska*, edited by Brown et al., Van Nostrand Reinhold, Stroudsburg, Pa.

Natural Resources Canada (1995), Map Canada - Permafrost, in *The National Atlas of Canada*, 5th ed., (Available at http://atlas.gc.ca/), Geol. Surv. of Canada, Natural Resources Canada, Ottawa, Canada.

NSIDC, National Snow and Ice Data Center (2003), *Circumpolar Active-Layer Permafrost System (CAPS)* [CD-ROM], Univ. of Colorado, Boulder, Colo.

Oechel, W. C., and B. Sveinbjörnsson (1978), Primary production processes in arctic bryophytes at Barrow, Alaska, in *Vegetation of Production Ecology of an Alaskan Arctic Tundra. Ecological Studies*, vol. 29, edited by L. L. Tieszen, Springer, New York.

Ohmura, A. (1982), Climate and energy balance on the Arctic tundra, *J. Climatol.*, *2*, 65–84.

Pfeiffer, E.-M., D. Wagner, S. Kobabe, L. Kutzbach, A. Kurchatova, G. Stoof, and C. Wille (2002), Modern processes in permafrost-affected soils, in *Reports on Polar Research*, *426*, Alfred Wegener Institute, Bremerhaven, Germany.

Priestley, C. H. B., and R. J. Taylor (1972), On the assessment of surface heat flux and evaporation using large-scale parameters, *Mon. Weather Rev.*, *100*, 81–92.

ROSHYDROMET (2006), Weather Information for Tiksi, (Available at http://www.worldweather.org/107/c01040.htm), Russian Federal Service for Hydrometeorology and Environmental Monitoring, Moscow.

Roth, K., R. Schulin, H. Flühler, and W. Attinger (1990), Calibration of time domain reflectometry for water content measurement using a composite dielectric approach, *Water Resour. Res.*, *26*, 2267–2273.

Rouse, W. R. (1990), The regional energy balance, *Northern Hydrol., NHRI Sci. Rep.*, *1*, 187–206.

Rouse, W. R., and R. B. Stewart (1972), A simple model for determining the evaporation from high latitude upland sites, *J. Appl. Meteorol.*, *11*, 1063–1070.

Rouse, W. R., P. F. Mills, and R. B. Stewart (1977), Evaporation in high latitudes, *Water Resour. Res.*, *13*, 909–914.

Schwamborn, G., V. Rachold, and M. N. Grigoriev (2002), Late quaternary sedimentation history of the Lena Delta, *Quat. Int.*, *89*, 119–134.

Smith, L. C., Y. Sheng, G. M. MacDonald, and L. D. Hinzman (2005), Disappearing Arctic lakes, *Science*, *308*(5727), 1429, doi:10.1126/science.1108142.

Soegaard, H., B. Hasholt, T. Friborg, and C. Nordstroem (2001), Surface energy- and water balance in a High-Arctic environment in NE Greenland, *Theor. Appl. Climatol.*, *70*, 35–51.

Spielhagen, R. F., H. Erlenkeuser, and C. Siegert (2005), History of freshwater runoff across the Laptev Sea (Arctic) during the last deglaciation, *Global Planet. Change*, *48*(1–3), 187–207, doi:10.1016/j.gloplacha.2004.12.013.

Stewart, J. M., and P. Broadbridge (1999), Calculation of humidity during evaporation from soil, *Adv. Water Resour.*, *22*(5), 495–505.

Stewart, R. B., and W. R. Rouse (1976), Simple models for calculating evaporation from dry and wet tundra surfaces, *Arct. Antarct. Alp. Res.*, *8*(3), 263–274.

Stewart, R. B., and W. R. Rouse (1977), Substantiation of the Priestley and Taylor parameter $\alpha = 1.26$ for potential evaporation in high latitudes, *J. Appl. Meteorol.*, *16*(6), 649–650.

USDA, United States Department of Agriculture, Natural Resources Conservation Service (1998), *Keys to Soil Taxonomy*, 8th ed., Soil Survey Staff, Washington, D. C.

Vörösmarty, C. J., L. D. Hinzman, B. J. Peterson, D. H. Bromwich, L. C. Hamilton, J. Morison, V. E. Romanovsky, M. Sturm, and R. S. Webb (2001), The hydrologic cycle and its role in arctic and global environmental change: A rationale and strategy for synthesis study, in *Arctic Research Consortium of the U.S.*, 84 pp., Arctic Research Consortium of the U.S., Fairbanks, Alaska.

Vourlitis, G. L., and W. C. Oechel (1997), Landscape-scale CO_2, H_2O vapour and energy flux of moist-wet coastal tundra ecosystems over two growing seasons, *J. Ecol.*, *85*, 575–590.

Vourlitis, G. L., and W. C. Oechel (1999), Eddy covariance measurements of net CO_2 and energy fluxes of an Alaskan Tussock tundra ecosystem, *Ecology*, *80*(2), 686–701.

Wagner, D., S. Kobabe, E.-M. Pfeiffer, and H.-W. Hubberten (2003), Microbial controls on methane fluxes from a polygonal tundra of the Lena Delta, Siberia, *Permafrost Perigl. Process.*, *14*, 173–185, doi:10.1002/ppp.443.

Wagner, D., A. Lipski, A. Embacher, and A. Gattinger (2005), Methane fluxes in extreme permafrost habitats of the Lena Delta: Effects of microbial community structure and organic matter quality, *Environ. Microbiol.*, *7*, 1582–1592.

Woo, M. K., and X. J. Guan (2006), Hydrological connectivity and seasonal storage change of tundra ponds in a polar oasis environment, Canadian High Arctic, *Permafrost Perigl. Process.*, *17*, 309–323.

Woo, M. K., and P. Marsh (1990), Response of soil moisture change to hydrological processes in a continuous permafrost environment, *Nord. Hydrol.*, *21*, 235–252.

Woo, M. K., and K. L. Young (2003), Hydrogeomorphology of patchy wetlands in the High Arctic, polar desert environment, *Wetlands*, *23*(2), 291–309.

Woo, M. K., and K. L. Young (2006), High Arctic wetlands: Their occurrence, hydrological characteristics and sustainability, *J. Hydrol.*, *320*(3–4), 432–450.

Yang, D., D. Kane, L. Hinzman, X. Zhang, T. Zhang, and H. Ye (2002), Siberian Lena River hydrologic regime and recent change, *J. Geophys. Res.*, *107*(D23), 46–94, 4694, doi:10.1029/2002JD002542.

Yoshikawa, K., and L. D. Hinzman (2003), Shrinking thermokarst ponds and groundwater dynamics in discontinuous permafrost near Council, Alaska, *Permafrost Perigl. Process.*, *14*, 151–160, doi:10.1002/ppp.451.

Young, K. L., and M. K. Woo (2000), Hydrological response of a patchy High Arctic wetland, *Nord. Hydrol.*, *31*(4/5), 317–338.

Zhang, T., R. G. Barry, K. Knowldes, J. A. Heginbottom, and J. Brown (1999), Statistics and characteristics of permafrost and ground-ice distribution in the northern hemisphere, *Polar Geogr.*, *23*(2), 132–154.

————————————

A. Abnizova, Department of Geography, York University, 4700 Keele Street, Toronto, Ontario, Canada M3J 1P3.

J. Boike, Periglacial Section, Alfred Wegener Institute for Polar and Marine Research, Telegrafenberg A43, 14473 Potsdam, Germany. (jboike@awi-potsdam.de)

C. Wille, Institute of Botany and Landscape Ecology, University of Greifswald, Grimmer Strasse 88, 17487 Greifswald, Germany.